Received: 5 May 2025 | Revised: 5 May 2025 | Accepted: 14 June 2025

DOI: 10.1111/cote.70007

FULL PAPER

Coloration Technology

Red era: Dyeing yak hair fibres red with in situ generated silver nanoparticles using silver nitrate and a flavonoid-containing plant extract

Julia K. Hachmann[1] | **Jule M. Sauler**[1,2] | **Charlotte Ruhmlieb**[1] | **Volkmar Vill**[1] | **Fabian Straske**[1,2]

[1]Department of Chemistry, University of Hamburg, Hamburg, Germany

[2]Henkel Consumer Brands, R&D Hair Color, Henkel AG & Co. KGaA, Hamburg, Germany

Correspondence

Fabian Straske, Henkel Consumer Brands, R&D Hair Color, Henkel AG & Co. KGaA, Ruhrstraße 19, 22761 Hamburg, Germany.
Email: fabian.straske@henkel.com

Funding information

Hamburgische Investitions- und Förderbank

Abstract

Plants and their extracts have been used for dyeing fabrics, skin and hair for thousands of years and have been experiencing a revival in the last years due to increasing health risks arising from oxidative hair dye precursors. We developed a novel two-step method to dye keratin fibres based on in situ formed silver nanoparticles including a flavonoid-containing plant extract from *Reseda luteola* L. and silver nitrate. Yak belly and human hair strands were treated with the aqueous plant extract, adjusted to pH 3 using hydrochloric acid (HCl) or citric acid (CA) or combined with sodium chloride (NaCl). In a second step, the keratin fibres were treated with a silver nitrate solution facing subsequent ultraviolet-visible (UV-visible) irradiation. The proposed method resulted in an intense and long-lasting red dye result, with over 85% colour retention after 24 washes. Microscope images of microtome cuts revealed an increase in penetration depth of the red colour of more than 10% after washing compared to unwashed strands, demonstrating the dye's longevity on and in the hair fibre. No mechanical damage of the hair fibre resulting from dyeing was depicted. The dye did not change the chemical composition of the hair surface as confirmed by X-ray photoelectron spectroscopy and Fourier-transform infrared spectroscopy. UV-visible spectra recorded during red dye formation in aqueous solution showed a peak at 450 nm being characteristic for surface plasmon resonance of silver nanoparticles. Transmission electron microscopy (TEM) images of dried nanoparticles isolated from solution were of a quasi-spherical shape with different sizes, ranging from 1 to 38 nm.

1 | INTRODUCTION

Plants and their extracts have been used for dyeing fabrics, skin and hair for thousands of years. Dye materials are used either exclusively (e.g., henna or indigo) or in combination with metal salts to alter and fixate the dye on the fabric.[1–4] When synthetic dyes were developed in the nineteenth century, they quickly became a commercial success and hence, naturally derived dyes sank into oblivion. Nowadays, the cosmetic industry faces a growing demand in more

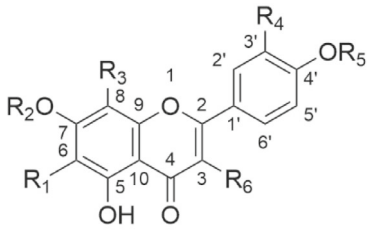
This is an open access article under the terms of the Creative Commons Attribution License, which permits use, distribution and reproduction in any medium, provided the original work is properly cited.
© 2025 The Author(s). *Coloration Technology* published by John Wiley & Sons Ltd on behalf of Society of Dyers and Colourists.

sustainable hair dye products.[4] Potential health risks arise from oxidative hair dye precursors, such as *para*-phenylendiamine (PPD). The molecule is known to cause allergies and its oxidised form was proven to be mutagenic in animal studies.[5] Furthermore, oxidative dye precursors are known for their negative impact on aquatic ecosystems.[6,7] Yet, especially red dye precursors, for example, 1-naphthol or 3-aminophenol,[8] are crucial for a majority of shades, controlling warmer or cooler tones. Thus, the search for a substitute places more emphasis on plant-derived hair colorations once again.

Anthocyanins, for example, derived from grapes, or alizarin, an anthraquinone dye derived from madder, are typical natural sources for red colour. The colour outcome of both anthocyanins and anthraquinones strongly depends on the pH value of the respective solution. For anthocyanins it varies from red in an acidic environment to purple-blue in an alkaline medium, whereas the red monovalent anion of alizarin is stable at a neutral to slightly alkaline pH.[9,10] Both compounds can thus be attributed to the "direct dyes", since they can be used exclusively to achieve a dye outcome. Due to the harsh acidic conditions that have to be applied in terms of anthocyanins, a lasting, intense red dye outcome on hair using anthocyanins has not been achieved yet, to the best of our knowledge. Besides, the thermal and light instability of anthocyanins makes their application as a substitute challenging. On the contrary, alizarin seems to show a more stable dye result on wool[11] and hair.[10] Yet, more data is required here regarding the longevity of the dye.

In this work, the focus of plant-derived hair colorations lies on the principle of combining plants and metal salts in order to achieve a dye result. This concept is based on the substance group of polyphenols, plants' secondary metabolites, responsible for the formation of coloured organic metal complexes. The plant of choice, *Reseda luteola* L. contains compounds of an important chemical group amongst polyphenols, namely flavonoids. The most frequent flavonoids, luteolin, apigenin and kaempferol are contained as glycosylated species as well as aglycones in the plant (Figure 1). These chromophores are responsible for dyeing fabrics in yellow shades and are traditionally rooted on fabrics in combination with alaun, an aluminium salt, to form polyphenol–alaun-complexes.[12,13] To expand the colour spectrum of *Reseda luteola* L. beyond yellow, metals salts can be varied.[14] A vibrant red does not belong to the portfolio yet.

Many research groups use wool as a fabric to investigate dyeing and mordanting with *Reseda luteola* L.[17–19] The application of silver nitrate ($AgNO_3$) in the process of mordanting wool is primarily known for its antibacterial purposes.[20] In terms of hair dyeing, individual plant-derived polyphenols have indeed been combined with metal salts to form complexes[21] or pigments[22] but only little research has been done regarding the use of plant extracts to dye human or animal hair. However, Sargsyan et al.[23] established a two-step method for dyeing hair using tannin-rich matcha tea with subsequent application of an iron(II)-salt. Based on the mordanting and complex-forming properties of tannins, an intense dark grey colour on human hair was achieved. In contrast, to the best of our knowledge, the use of *Reseda luteola* L. to dye hair has not yet been shown before.



Structure	R1	R2	R3	R4	R5	R6
Luteolin	H	H	H	OH	H	H
Luteolin-7-*O*-glucoside	H	Glucose	H	OH	H	H
Luteolin-3',7-*O*-glucoside	H	Glucose	H	O-Glucose	H	H
Apigenin	H	H	H	H	H	H
Apigenin-7-*O*-glucoside	H	Glucose	H	H	H	H
Apigenin-6,8-di-*C*-glucoside	Glucose	H	Glucose	H	H	H
Kaempferol	H	H	H	H	H	OH
Kaempferol-3-*O*-glucoside-7-*O*-rhamnoside	H	Rhamnose	H	H	H	Glucose

FIGURE 1 Flavonoid structures of *Reseda luteola* L. including the aglyconic structures luteolin, apigenin and kaempferol as well as their most common glycosylated structures.[15,16]

Moreover, polyphenols show a reductive potential, enabling them to form nanoparticles (NPs) from metal ions. The polyphenol-based formation of silver nanoparticles (AgNPs) using alcoholic plant extracts, including *Reseda luteola* L.[24] has been shown by various research groups and allows for a less toxic way to yield NPs compared to former methods.[25–27] Accordingly, polyphenolic compounds act as reducing agents for silver ions, while further plant ingredients stabilise the resulting AgNPs preventing them from agglomeration.[26]

Up to now, NP formation based on hair as substrate is known from research projects, in which the application of toxic chemicals during the formation process shall be avoided. NPs are grown on the hair's surface, extracted and used for further purposes such as nanocatalysts.[28,29] Preparation of NPs with the intention of dyeing hair was first tackled by Haveli et al.[30] The group prepared gold nanoparticles (AuNPs) in situ inside human hair using chloroauric acid ($H[AuCl_4]$) in an alkaline medium. Tang et al.[31] used gallic acid, a phenolic acid, to reduce silver ions and to deposit resulting AgNPs on diatoms for subsequent hair dyeing. Until now, no method is described in the literature using a combination of a plant extract rich in polyphenols and a $AgNO_3$ solution for hair dyeing.

In this work, we showed a two-step hair dye method with subsequent light irradiation to achieve a red dye result on hair fibres ascribed to in situ NP formation and thus taking the hair to the red era of plant-based hair coloration. At first, a combination of an aqueous suspension of *Reseda luteola* L. plant extract (RE) and an additive was used followed by $AgNO_3$ in the second step. The additive was either 5% sodium chloride (NaCl) or hydrochloric acid (HCl) or citric acid (CA), respectively, for pH adjustment of the plant extract. The dye outcome depending on the additive as well as the intensity were scrutinised using spectrophotometric measurements and standardisation via CIELab colour space. Additionally, we could emphasise the longevity of the dye result via wash fastness tests and cross-sections of hair fibres. The impact of the dye and subsequent washing procedure on chemical composition and mechanical behaviour of the fibre was investigated using X-ray photoelectron spectroscopy (XPS) and Fourier-transform infrared (FTIR) spectroscopy as well tensile testing. For a better understanding of the AgNP formation, ultraviolet-visible (UV-visible) spectra of in-vitro synthesised AgNPs were recorded.

2 | EXPERIMENTAL

2.1 | Materials

Yak belly hair tresses as well as blonde tresses from European human hair were obtained from Kerling International Haarfabrik GmbH, Backnang, Germany. Yak tresses had a total length of 11.8 cm of which 7.5 cm included hair fibres and a weight of fibres of 0.70 g. Yak belly hair is naturally white and required no bleaching prior to use granting optimal dye results. The human hair tresses had a total length of 10 cm of which 8 cm included hair fibres and a weight of 0.40 g. They were deep-cleansed, but not bleached by the manufacturer. Ultrapure water (UPW) was used throughout all experiments. The purification was conducted using the Arium Pro Ultra-Pure Water System from Sartorius AG, Göttingen, Germany. Before dyeing, all hair strands were precleansed according to the following method to wash off potential residues from the manufacturing process and to guarantee equal starting conditions regardless of different batches: The strands were wetted at room temperature (r.t.) with a total UPW flow of 25 mL s^{-1} and placed in 20 mL per strand of an aqueous 12.5% sodium laureth sulphate (SLES) solution adjusted to pH 4.5 using 20% sulphuric acid (H_2SO_4 98%, CAS: 7664-93-9), purchased from Merck KGaA, Darmstadt, Germany, freshly diluted in the laboratory, for 30 min. It was made sure that the strands were fully covered in the cleansing bath. The strands were subsequently rinsed twice with UPW at a total flow of 25 mL s^{-1}, combed 20 times and air-dried. The strands were used without any further pretreatment.

2.2 | General dyeing method using *Reseda luteola* L. and $AgNO_3$

All investigations were conducted using a hydroalcoholic extract powder of aerial flowering parts of *Reseda luteola* L., kindly provided by Couleur de Plantes (Rochefort, France). The plants were harvested in France in August 2013 and extracted in November 2022. $AgNO_3$ (CAS: 7761-88-8) was purchased from Carl Roth, Karlsruhe, Germany; NaCl (99.5%, CAS: 7647-14-5) was purchased from Grüssing GmbH, Filsum, Germany; H_2SO_4 (95–97%, CAS: 7664-93-9) was purchased from Merck KGaA, Darmstadt, Germany; anhydrous CA (CAS: 77-92-9) was purchased from Inter-Harz GmbH, Klein-Offenseth-Sparrieshop, Germany; HCl (37%, CAS: 7647-01-0) was purchased from VWR International GmbH, Darmstadt, Germany. Aqueous dilutions to concentrations of HCl 10% were freshly prepared in the laboratory. The additives used were of analytical grade.

The dyeing was conducted in a two-step process as follows, modified after Sargsyan et al.[23]

For each strand receiving a combinatory treatment of RE and one additive, for the first step, 500 mg RE were suspended in 50 mL of UPW, to obtain an aqueous RE

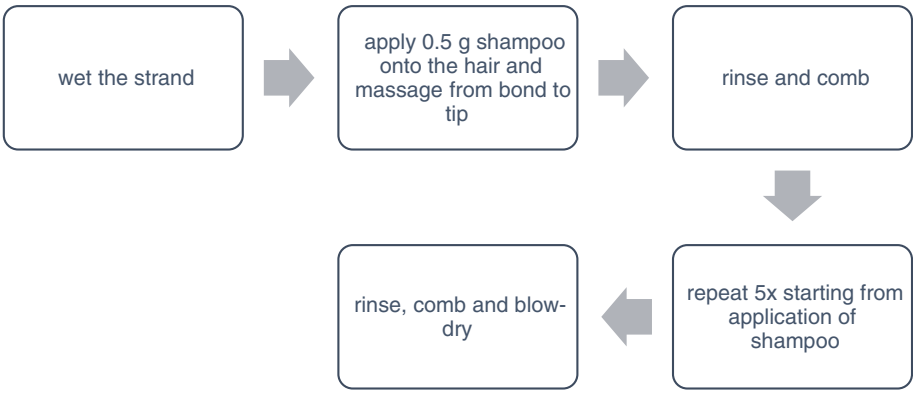


FIGURE 2 Visualisation of method for wash fastness tests comprising five consecutive steps. After wetting the strands in the first step, steps two and three are conducted six times in total followed by a final rinse, comb and blow-dry step.

suspension (1% w/v) with a natural pH of 5.30. The suspension was then mixed with either 5% NaCl or the pH was adjusted to 3 using 10% HCl(aq.) or CA. The strands were stirred in the suspension at r.t. for 30 min. The control strand (nat. pH, w/RE) received no further additive.

For each strand treated without RE, 50 mL of an aqueous solution only containing one of the earlier-mentioned additives was prepared and the strands were stirred for 30 min accordingly. The control strands (nat. pH, w/o RE) were stirred in UPW at r.t. for 30 min for comparability.

Afterwards, the strands were rinsed at r.t. with a total UPW flow of 25 mL s^{-1}, combed 20 times and blow-dried with a commercially available blow-dryer.

In a second step, 500 mg $AgNO_3$ per strand were dissolved in 50 mL UPW (1% w/v) and the pre-treated strands were stirred at r.t. for 10 or 30 min under exclusion of light. The strands were again rinsed, combed and blow-dried as described earlier. Subsequently, the strands were irradiated under a PAR38 full-spectrum plant-lamp (euroLighting GmbH, Nagold, Germany), emitting UV-visible radiation within 390–780 nm. A detailed spectrum tackling light intensity measurements is attached in Supporting Information Figure S1. The light intensity was measured using the OHSP-350 Portable Spectral Irradiance Colorimeter (Hangzhou Hopoo Light&Colour Technology Co., Ltd, China). The distance between light source and strands was 35 cm and the strands were kept inside the closed chamber for at least 5 h.

2.3 | Method of wash fastness testing

To determine the wash stability of the hair dye as a quality feature, yak belly strands were wetted at r.t. with a total UPW flow of 25 mL s^{-1} and washed up to 24 times (four wash cycles) using the commercially available Schauma 7 Kräuter Shampoo (Schwarzkopf, Düsseldorf, Germany). One wash cycle comprised six washes of 0.5 g shampoo. The shampoo was massaged into the strands 10 times from bond to tip. Afterwards, the strands were rinsed with a total waterflow of 25 mL s^{-1} and combed. The procedure was repeated five times. After the last rinse, the strands were blow-dried (Figure 2).

2.4 | General method of NP synthesis from *Reseda luteola* L. extract and $AgNO_3$

The synthesis of AgNPs was performed according to the method of Singh et al[25] using slight modifications. A stock solution of RE in UPW was prepared using 339 mg RE suspended in 50 mL UPW (6.78 mg mL^{-1}). After 10 min of stirring at 200 rpm, the solution was filtered through 0.22 µm polyvinylidene difluoride (PVDF) membranes (VWR International GmbH, Darmstadt, Germany). A stock solution of $AgNO_3$ was prepared at 40 mmol L^{-1} in UPW. For AgNP synthesis, 5 mL of RE stock solution was diluted to 47 mL and mixed with 3 mL of $AgNO_3$ stock solution to a final concentration of 2.40 mmol L^{-1} $AgNO_3$ and 0.678 mg mL^{-1} RE. To start the reaction, the solution was exposed to UV-visible radiation for 1 h.

2.5 | Processing of hair strands for analytics

The determination of silver content in hair strands required a uniform sample and a high level of surface area, preferably a powder. Thus, yak belly strands were ground using a Pulverisette 23 ball mill (Fritsch GmbH, Idar-Oberstein, Germany), equipped with a zirconium oxide grinding bowl and balls. The runtime was 2 × 5 min with a cool-down time of 2–3 min in between and a frequency of 50 s^{-1}.

2.6 | Determination of silver-load on hair strands

In order to determine the amount of silver on the hair strands, elemental analysis was conducted using ARCOS

ICP-OES analyser (Spectro Analytical Instruments GmbH, Kleve, Germany). The ground hair samples were refluxed in aqua regia (1:3 nitric acid to HCl) at 160°C for 2 h and diluted subsequently for analysis.

2.7 | Microtome-cuts for microscopy and determination of penetration depth

To determine the penetration depth of the dye, cross-sections of yak belly hair fibres were cut at the Henkel AG & Co KGaA site (Düsseldorf, Germany) using the Epredia NX70 with Vakutom (Leica Biosystems Nussloch GmbH, Nussloch, Germany). The hair samples were embedded in Tissue Freezing Medium (Leica) and were frozen to −50°C. Subsequently, the fibres were cut at −16°C and a knife temperature of −23°C to a thickness of 3 µm. The cuts were finally fixed between glass plates.

Microscopic images were taking using an Olympus BX51 fluorescence microscope and an Olympus DP71 digital microscope camera (Olympus Europa SE & Co. KG, Hamburg, Germany).

The relative penetration depth in percentage describes the penetration of hair dye in relation to the diameter of the hair and is defined as:

$$\text{Relative penetration depth}(\%) = \frac{\text{abs. penetration depth}(\mu\text{m})}{\text{hair diameter}(\mu\text{m})} \times 100$$

Since the hair is not of a perfectly spheric shape, the relative penetration depth was calculated both for the smallest and largest hair diameter of the fibre and is thus depicted as a range.

2.8 | Spectrophotometric measurement using DataColor

For objectification of dyes, yak belly strands were measured spectrophotometrically using a DataColor SF600 Spectraflash device to obtain L^*, a^* and b^*-values/coordinates according to the CIELab three-dimensional colour space. The L^*-value defines brightness (0 = black, 100 = white), a^* defines the red-green coordinate and b^* the blue-yellow coordinate. The values were taken after colour development was completed.

The spectral reflectance recorded was converted into colorimetric data using DCI colour software. Each strand was measured four times, altering the angle by 90° after each measurement.

Colour differences are expressed using the ΔE value, which is defined as[32]:

$$\Delta E = \sqrt{\left((L_1{}^* - L_2{}^*)^2 + (a_1{}^* - a_2{}^*)^2 + (b_1{}^* - b_2{}^*)^2\right)}$$

The ΔE value was calculated with the mean of five undyed strands for L_1^*, a_1^* and b_1^*.

2.9 | Characterisation of elemental composition and chemical bond changes of hair surface

In order to examine the elemental composition as well as chemical bond changes on the hair surface before and after dyeing, as well as after washing, XPS was conducted using an ESCALAB 250Xi (GSOP-00344) (Thermo Fisher Scientific Inc., Waltham, MA, USA) equipped with an aluminium-mono anode at a sampling area of 400 microns.

To assess the amount of cysteic acid inside the hair fibre, FTIR spectroscopy was performed on a MPA FT-NIR spectrometer (Bruker Optics GmbH & Co. KG, Ettlingen, Germany) with an integrating sphere module at six different sample positions in diffuse reflection, covering a wavenumber range from 7300 to 4020 cm^{-1}.

2.10 | Impact of dye and subsequent washing procedure on hair stress and strength

To assess the potential impact of the dye and subsequent washing on hair structure affecting hair stress and strength, investigations regarding tensile elongation were conducted using a tensile testing device BTC-FR1.0TH. D09 (ZwickRoell GmbH & Co. KG, Ulm, Germany). The grip-to-grip separation was 44 mm, the test speed was 50 mm min^{-1} and the pre-load was 0.1 MPa. The experiments were conducted at 23.5°C and 19% relative humidity (RH). The diameter of the hair was determined at three spots of the fibre using scanning electron microscopy (SEM). One hair fibre was fixed between the jaws that were supported using a polymer tape for additional grip. The fibre did not come into contact with the glue. After securing the fibre at both ends, the device was steadily pulled until failure of the fibre. Values for break force (N) and strain (%) were collected. Only results from fibres that ripped within the middle 50% of the length of the fibre were considered for statistical analyses.

Hair stress (MPa) is defined as[33]:

$$\text{Hair stress (MPa)} = \frac{\text{Break force (N)}}{\text{cross sectional area (mm}^2\text{)}}$$

Hair strain is defined as[33]:

$$\text{Hair strain} = \frac{\text{elongation of fibre}}{\text{original length}}$$

Young's modulus (GPa) in the elastic region was calculated with[33,34]:

$$\text{Young's modulus (GPa)} = \frac{\Delta\sigma}{\Delta\epsilon}$$

where σ defined the change in stress and ϵ the change in strain.

2.11 | UV-visible spectrophotometric measurements of NP suspension

Spectrophotometric measurements of in-vitro synthesised AgNPs were carried out at r.t. using a Lambda 365+ UV-visible-spectrophotometer (PerkinElmer LAS GmbH, Rodgau, Germany) equipped with UV WinLab software. The UV-visible spectra were recorded from 200 to 700 nm using quartz cuvettes (1.00 cm light path, purchased from Carl Roth GmbH + Co. KG, Karlsruhe, Germany). Spectra of the following samples were recorded: $AgNO_3$ solution (2.4 mM), RE solution (0.678 mg mL^{-1}) and AgNP suspension. Samples were diluted 1 to 4 prior to measurement. Either UPW or RE solution (0.678 mg mL^{-1}, diluted 1 to 4) served as blanks. Data evaluation was performed using OriginPro 2022 Software (OriginLab Corporation, Northampton, MA, USA).

2.12 | Transmission electron microscopy (TEM)-images of dried AgNPs

For evaluation of size and shape of AgNPs, transmission electron microscopy (TEM) was performed using a JEOL JEM 1011 at an acceleration voltage of 100 kV (JEOL Germany GmbH, Freising, Germany). The AgNP samples were prepared by drop coating the AgNP suspensions on carbon coated copper TEM grids. The software programs OriginPro 2022 and ImageJ 1.53t were used for data evaluation.

2.13 | Statistical analysis

Statistical analysis was performed using IBM SPSS Statistics version 29.0 (IBM Corp., Armonk, NY, USA). Descriptive statistics, comprising mean value and standard deviation (SD) were collected. Results are presented as mean ± SD. In figure 5, the results are presented as error bars ± two times SD. Independent samples *t*-test for equal and non-equal variances were performed at a critical significance level of $p = 0.05$ to assess the differences in hair stress, strain and Young's modulus between undyed, dyed as well as dyed and washed strands.

3 | RESULTS AND DISCUSSION

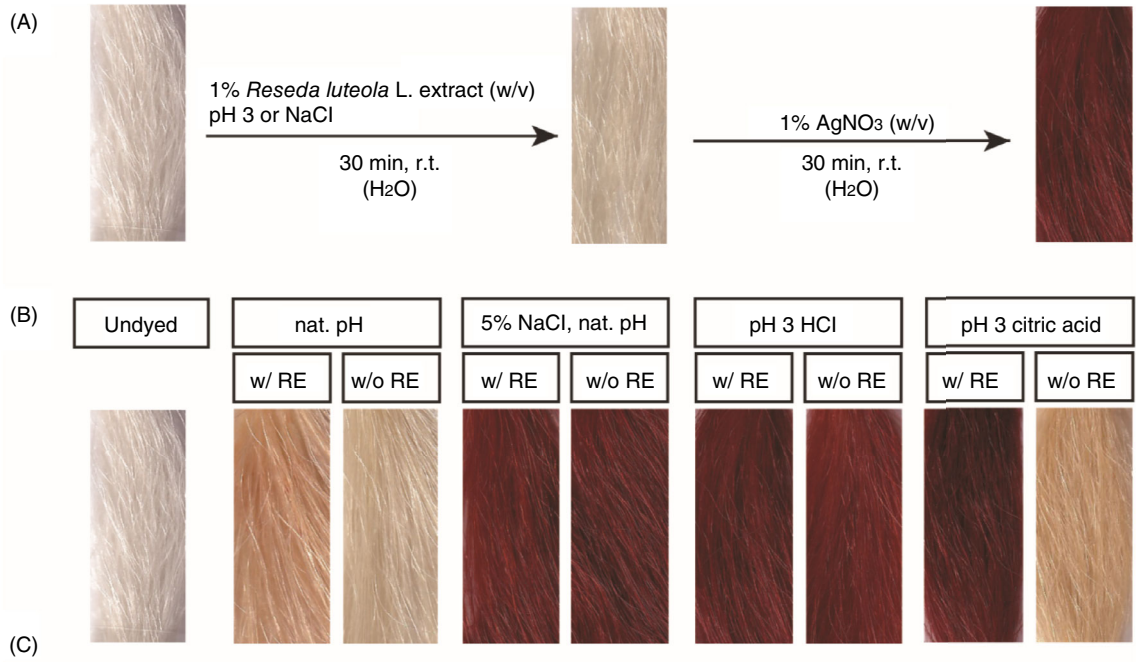
3.1 | Influence of additive on dye outcome

The treatment of yak belly hair strands according to the two-step-method with 1% RE suspension first and 1% $AgNO_3$, subsequently, resulted in intense red dye results upon irradiation (Figure 3A). The combination of NaCl and RE suspension or its adjustment to pH 3 via HCl or CA was crucial for the dye outcome since no colour developed in control strands, when dyeing was conducted at the natural pH value of 5.30 of RE (Figure 3B) or when 1% $AgNO_3$ was used without preliminary RE treatment. The addition of 5% NaCl to the RE suspension, followed by 1% $AgNO_3$ treatment led to a red colour result on the strands, with a ΔE of 53.3 ± 2.4 compared to undyed strands (Figure 3B,C). Strands treated with the RE suspension at pH 3 adjusted using HCl or CA, respectively, and 1% $AgNO_3$ subsequently, also yielded an intense red colour after the dyeing and colour development process was completed, represented by a shift in ΔE of 56.0 ± 1.2 and ΔE of 56.0 ± 2.2, respectively. Contrary, strands treated with 1% RE suspension at the natural pH value (pH 5.30) and 1% $AgNO_3$ solution subsequently, solely showed a slight shift in colour towards a reddish hue after 5 h of colour development, depicted by a ΔE of 21.1 ± 2.5. A permanent light irradiation of at least 5 h is required to obtain the final dye results described. Control experiments of strands that were irradiated for only 10 min and kept under light exclusion for up to 5 h, did not develop the intense dye result, but only a pale rose. Hence, the reaction was not "cascade-like", but needed constant irradiation for a uniform dye result.

Furthermore, the application of either HCl or NaCl exclusively, followed by 1% $AgNO_3$ treatment also induced the development of red colour. Strands treated without RE at pH 3 adjusted using HCl prior to the $AgNO_3$ treatment showed a ΔE of 53.6 ± 1.6, comparable to the strand with RE (ΔE of 56.0 ± 1.2). Strands treated with 5% NaCl solution followed by 1% $AgNO_3$ resulted in a ΔE of 54.1 ± 1.6. No difference in colour outcome was depictable compared to the treatment with RE (ΔE of

53.3 ± 2.4). The influence of chloride on the dye outcome was clearly evident. Hence, the slight colour shift observed on strands treated with 1% RE suspension at a natural pH followed by 1% $AgNO_3$ solution could therefore possibly be ascribed to a certain chloride content already present in the extract or synergistic effects of RE and naturally contained chloride.

Hair strands treated with RE, adjusted to pH 3 with CA prior to $AgNO_3$ treatment, developed a colour result (ΔE of 53.7 ± 0.8), whereas strands treated without RE, but adjusted to pH 3 using CA prior to $AgNO_3$ treatment, showed no colour development at all after 5 h of irradiation (ΔE of 15.3 ± 0.7). These findings further underlined the role of RE and its synergistic effect with CA and $AgNO_3$ in the absence of chloride. CA was chosen based on its relevance for cosmetic applications. The results were substantiated by the use of further cosmetic-related acids such as malonic acid, succinic acid, malic acid or acetic acid (Figure S2). With all these acids used, RE was essential for colour development. Besides, strands solely treated with 1% $AgNO_3$ showed no colour development either after 5 h of irradiation (ΔE of 9.8 ± 1.3). Likewise, 1% RE suspension applied exclusively without $AgNO_3$ did not result in the development of a red dye result, since the polyphenols adsorbed onto the hair's surface did not show a colour visible to the human eye (Figure 3A). Hence, neither an acidic milieu was sufficient solely, nor an interaction between silver ions and keratin fibres



(C)

Color coordinates	Dyeing conditions of hair strands in regards to plant extract and additive (n=3)								
	undyed	nat. pH (cont.)		5% NaCl, nat. pH		pH 3 HCl		pH 3 citric acid	
	-	w/RE	w/o RE	w/RE	w/o RE	w/RE	w/o RE	w/RE	w/o RE
L*	77.1±0.7	63.2±1.2	75.2±1.2	28.7±3.1	27.4±3.0	26.0±2.6	30.1±2.1	25.1±3.7	69.0±1.6
a*	-0.5±0.1	6.9±2.6	-0.8±0.1	20.7±1.7	20.1±2.3	20.8±0.9	23.8±0.6	20.0±2.5	3.2±0.5
b*	8.8±0.6	22.8±1.7	18.4±1.6	15.0±1.8	13.0±3.2	13.2±1.1	17.4±1.6	13.0±3.4	21.3±0.6
ΔE	-	21.1±2.5	9.8±1.3	53.3±2.4	54.1±1.6	56.0±1.2	53.6±1.6	56.1±2.2	15.3±0.7

FIGURE 3 (A) Schematic overview of hair dyeing procedure for yak belly strands. Treatment with 1% RE suspension shows no visible dye result on hair strand regardless of additive applied. Subsequent treatment with 1% $AgNO_3$ results in intense red dye outcome. (B) Yak hair tresses dyed w/ and w/o RE at natural pH, with 5% NaCl at the natural pH and acidified to pH 3 using HCl or CA and treated with 1% $AgNO_3$ subsequently. Hair strands treated with 1% RE suspension (w/RE) at the natural pH do not develop a red dye result. The treatment of hair fibres using only $AgNO_3$ (w/o RE) does not yield a red dye result either. Hair strands treated with a chloride-containing additive (5% NaCl or pH 3 HCl) show a red dye result after irradiation regardless of the addition of 1% RE suspension. When CA is used for acidification, a red dye result only develops in combination with 1% RE suspension. (C) L^*, a^*, b^*-values as well as ΔE-values including SD for yak hair tresses dyed w/ and w/o RE compared to an undyed strand.

alone was responsible for the dye result. With regard to the applicability for hair dye products and different hair types, these findings were confirmed using human hair (Figure S3). Similar results were observed, indicating that overall, the dye outcome was either achieved with chloride, regardless of the presence of RE or in combination of an acidic milieu and RE.

In the present case, electron-donating polyphenols potentially reduced electron-accepting silver(I) ions in the presence of HCl or NaCl with subsequent formation of NPs, resulting in the red dye outcome. King et al. found that palladium (Pd) ions could be reduced to Pd(0) with subsequent NP formation when a halide such as NaCl was present.[35] The bridging ligand effect of halides facilitated the electron transfer process between an electron-donating source and an electron-accepting compound. Another potential route of AgNP formation involves silver chloride (AgCl) as intermediate. In this case, $AgCl_x^{(x-1)}$ complexes act as precursors for AgNP synthesis under simulated sunlight irradiation.[36] The AgCl microcrystals further facilitated the formation of AgNPs.[37] The formation of highly insoluble AgCl in the first place seems very likely when NaCl and $AgNO_3$ are used exclusively on strands. The AgCl deposited on the strands surface subsequently reduces to AgNP under light irradiation involving the oxidation of chloride to chlorine.[38] Gummer depicted AgCl even within the hair's cuticula that in the context of his experiments interacted with $AgNO_3$ applied afterwards.[39] By contrast, CA alone could not reduce silver ions in the present case, despite its reductive properties.[40] But, it is also described that the reductive capacities of citrate are rather weak and more prominent at higher temperatures[41] compared to its stabilising properties of AgNPs.[42] This could explain why the strand treated only with CA and $AgNO_3$ remained colourless and required polyphenols from RE as a reductive agent. Probably compounds from both, RE extract and CA, synergistically took over stabilisation, as reported in the literature,[41] superseding chloride in the system. Since 5% of chloride and more, lower the viscosity in aqueous formulations and thus complicate the gelling and formulation of a consumer-pleasing application,[43] the application of CA as the acidifier was of increased interest, since the mechanism worked without chloride. Despite reported capping properties of keratin in the stabilisation of AgNPs,[44,45] this phenomenon could not be observed in the present work. In a strand that was treated with RE as a reductive agent without CA or chloride, keratin could not take over this role and the strand remained colourless.

3.2 | Affinity of silver towards hair

The amount of silver contained in the hair strand was almost identical regardless of the pre-treatment and dye outcome (Table 1). Ground hair samples were submitted to elemental analysis to determine the silver content and thus to investigate the affinity of silver ions towards hair fibres depending on the presence of RE and observed dye result. Samples, formerly treated solely with 1% $AgNO_3$ for 30 min, were composed of 3.3 ± 0.2% silver and samples formerly treated with 1% RE suspension prior to 1% $AgNO_3$ treatment, was composed of 3.0 ± 0.2% silver. It is important to note that the silver content found did not match a specific silver species, it could either be derived from silver ions or a reduced form of silver (bulk silver or NPs).

TABLE 1 Silver content in hair fibres in percentage and standard deviation (SD) dyed at nat. pH w/o RE and at nat. pH w/RE as well as w/RE at pH 3 using hydrochloric acid (HCl). The contents were determined from ground hair with elemental analysis.

Silver load on hair fibres dyed at different conditions in w % ($n = 3$)		
w/o RE nat. pH	**w/ RE nat. pH**	**w/ RE pH 3 HCl**
3.3 ± 0.2	3.0 ± 0.2	2.9 ± 0.1

There was no difference between the silver content on hair strands that were pre-treated with RE and those which were not treated with RE. Furthermore, red dye strands did not show a higher silver content either. A ground hair sample formerly treated with 1% RE suspension at pH 3 prior to 1% $AgNO_3$ treatment, was composed of 2.9 ± 0.1% silver. In the context of this work's sample, this marked the lowest amount of silver deposited on hair on an average. The difference in silver content in all three hair samples tested was negligible, but the results illustrated that the dye intensity was not a sufficient indicator for the amount of silver on hair. Moreover, it can be concluded that silver deposited on hair did not automatically react and develop a colour, but that a reactant was required. Bate[46] could show that silver ions tightly adsorb to the hair's surface with increasing pH-value, whereas here, silver was deposited on hair regardless of the pre-treatment showing that neither pH adjustment nor the use of RE could genuinely enhance or decrease hair's affinity for silver. It is known that ions penetrate the cortex regardless of charge due to their small size, complemented by sulphur-containing functional groups of keratin and their affinity for silver.[47]

Since the specific silver compounds could not be ascertained using elemental analysis, the exact amount of silver relevant for the dye outcome could not be concluded from the results. It is assumed that a certain amount of AgCl precipitated due to its low solubility



Color coordinates	Strand dyed at pH 3 HCl w/RE (n=3)	
	10 mins	30 mins
L*	26.3±1.7	26.0±2.6
a*	20.7±0.2	20.8±0.9
b*	12.9±0.1	13.2±1.1
ΔE	55.1±1.7	56.0±1.2

FIGURE 4 Visual comparison of strands treated with $AgNO_3$ for either 10 or 30 min. No differences were depicted. The L^*, a^*, b^* and ΔE values of corresponding strands. The values do not differ accordingly.

when NaCl or HCl were used as an additive, which was included in the amounts depicted earlier.

3.3 | Investigation of strands' exposition time to $AgNO_3$ on the dye outcome

The results did not depict differences in dye outcome for strands treated with $AgNO_3$ either for 10 or for 30 min (Figure 4). To optimise the dyeing method regarding exposure time of a hair strand towards $AgNO_3$, the time factor was evaluated. A strand treated with RE at pH 3 (HCl) and 1% $AgNO_3$ subsequently for a reduced time of 10 min, compared to the formerly established dyeing time of 30 min, showed an intense red colour, represented by a ΔE value of 55.1 ± 1.7 (Figure 4). Comparison of ΔE value with a strand stirred for 30 min in the $AgNO_3$ bath showed no visually noticeable difference. Each L^*, a^* and b^* values behave accordingly. Thus, stirring the strand in the $AgNO_3$ dye bath for 10 min was sufficient for an intense dye outcome.

3.4 | Wash fastness of strands dyed with RE at pH 3 (HCl)

Wash fastness tests conducted with dyed strands showed that overall, even 24 washes did not have a visible impact on the dye intensity (Figure 5A). Strands treated with RE at pH 3 (HCl) and 1% $AgNO_3$ subsequently were used for wash fastness experiments. After 6 washes, a grey veil was washed off the strands, hence they appeared more vibrant. This observation was represented by an increase in each, L^*, a^* and b^* values (Figure 5B) compared to an unwashed strand. After 12 and 18 washes, the strands showed no further considerable changes in colour intensity, demonstrated by only minimal shifts in L^*, a^* and b^* values. A plateau was reached after 18 washes for brightness L^*, indicating that no considerable amounts of dye were washed off hereafter. For a^* and b^* values solely slight increases were depicted after 18 washes, invisible to the human eye. The visual impression as well as calculated L^*, a^*, b^* and ΔE values (Supporting Information Table S1) suggest that for the overall dye outcome, no significant amounts of silver were washed off the hair during the wash cycles, but that the dyed strands benefited from washing since they appeared more vibrant. Additional elemental analysis of a ground sample of a previously washed strand revealed a silver content of 2.3 ± 0.1%. The results depicted that silver did come off the hair fibre compared to an unwashed strand (2.9 ± 0.1%), but that the amount was negligible for the dye perception. Since the exact silver species could not be determined in elemental analysis, as previously described, a mixture of mainly loosely attached AgNPs close to the surface or by-products such as residual AgCl might have been affected.

Cross-sections of hair fibres further illustrated the high wash fastness (Figure 6). With increasing numbers of washes, the penetration depth of the red dye enhanced. The average initial penetration depth of the red dye into strands treated with 1% RE at pH 3 and subsequent $AgNO_3$ treatment for 30 min. was determined to be 9.3 ± 1.7 µm. Considering the hair's diameter, this corresponded to a relative penetration depth of 10–14%. The penetration pattern resembled the ring-dye effect of demi-permanent hair dyes, substantiating the high wash fastness.[8] The penetration depth of the red dye increased after six washes (13.7 ± 3.0 µm, 14–17%). This result suggested that the first contact of the hair fibre with water and a surfactant after the dyeing process induced a mobilisation of the dye pointing inwards. Further increases in penetration depth were depicted after 12 washes (18.9 ± 4.2 µm, 19–23%) and 18 washes, reaching the highest penetration depth of 20.8 ± 3.2 µm and a relative penetration depth of up to 27%, respectively. The dye pattern at this point resembled multiple concentric dye rings. After 24 washes, the penetration depth slightly decreased, still resulting in an average depth of 14.6 ± 6.7 µm and 18–23%, respectively. Again, multiple concentric dye rings were observed.

The results showed a continuous penetration of the red dye into the hair fibre under the influence of water until up to 18 washes. Several factors need consideration

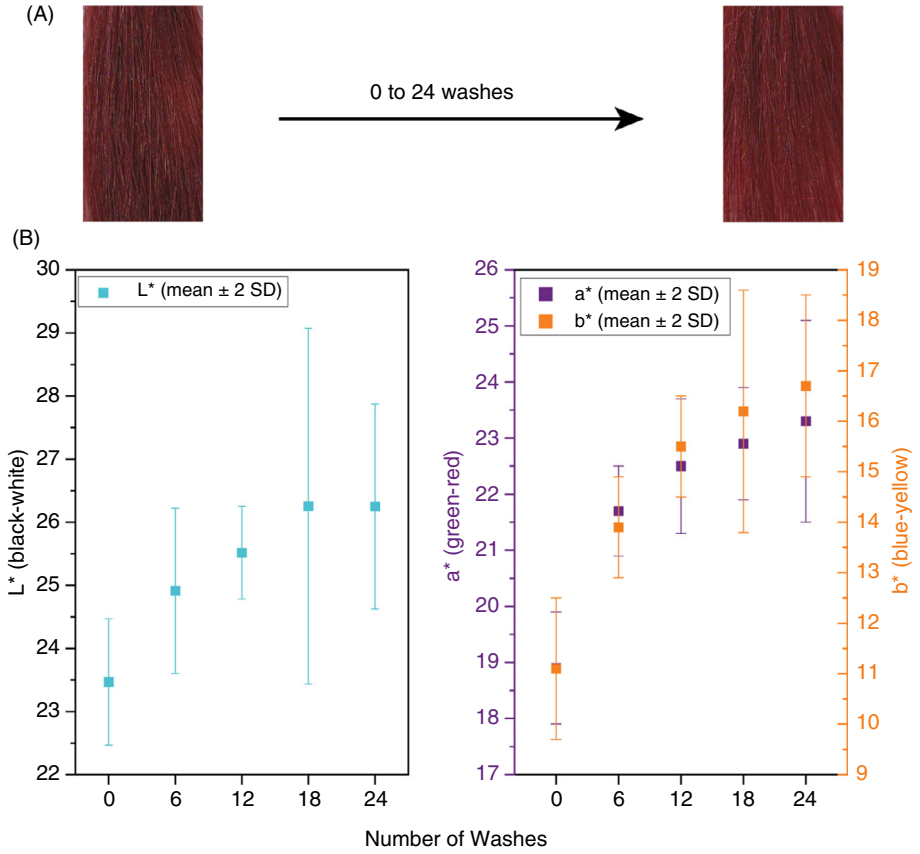
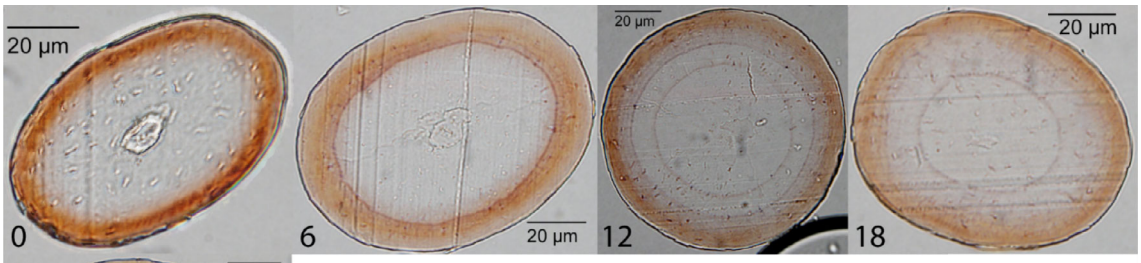


FIGURE 5 (A) Visual differences of a strand treated with RE at pH 3 (HCl) with subsequent $AgNO_3$ treatment before and after 24 washes. The wash process did not have a visible impact on the dye intensity. (B) Mean values and 2 SD for brightness (L^*) and colour hue (a^*, b^*) of earlier-mentioned strands before and after 24 washes ($n = 3$). The L^*, a^* and b^* values increased after each wash cycle (exception: L^* value after 18 washes) which resulted in a more vivid appearance of the strand. Corresponding ΔE values are annexed in Supporting Information Table S1.



	Number of washes, strand pH 3 HCl (n=5)				
	0	6	12	18 (n=4)	24
Penetration depth (µm) $\bar{x}$	9.3±1.7	13.7±3.0	18.9±4.2	20.8±3.2	14.6±6.7
Relative penetration depth (%)	10-14	14-17	19-23	21-27	18-23

FIGURE 6 Microscopic images of microtome cuts from strands before, after 6, 12, 18 and 24 washes. Concentric dye rings formed during the washing process and the dye penetrated deeper into the hair fibre with washing. Penetration depth (µm) depicts the absolute penetration and SD of the dye into the hair without appreciating the hair's irregular shape. The relative penetration depth in % describes the penetration in relation to the diameter of the hair, represented in a range from the smallest to the biggest diameter. Each five strands were investigated for 0, 6, 12 and 24 washes. One strand was excluded at 18 washes as an outlier.

as potential contributors to the effect. It is known that repeated contact of hair fibres with water causes swelling of the rigid hair fibre, making it easier for molecules and particles to penetrate.[48] Small pores found in yak hair potentially facilitate the movement of particles as they increase its porosity.[49] It is also conceivable that the water content might have remained at an increased level in deeper layers of the hair[50] compared to unwashed hair despite blow-drying in between the wash cycles, thus enabling further movement. Surfactants, such as SLES in shampoo used, further decrease the surface tension and promote the process. As a side effect, the swelling of hair fibres makes it easier for SLES to penetrate the fibre again.[51] NaCl as a gelling agent of the shampoo, as well as CA for pH adjustment, both depict genuine dye precursors that were introduced during the wash procedure. Concluding, the repetitive water contact, might have brought red dye particles, as well as precursors for AgNP formation, such as AgCl, NaCl or CA, deeper into the fibre. Complemented by a constant release of silver ions from the surface of existing NPs[52] into water that remained in deeper layers of the hair fibre, the reaction area expanded and more AgNPs formed.

Interestingly, after 24 washes, the dye impression seemed to relocate to the outer layers of the hair again, indicated by a more intense and compact dye ring at the outer layers compared to a thinner and faded dye ring after 18 washes (Figure 6, 18 and 24 washes). Considering the presumable highest water content in deeper areas of the fibre and the more compact dye ring after 24 washes, the effect might have just been due to evaporation of the remaining water, carrying the particles outwards. The air-drying process of hair can take up to several hours[53,54] and the cuts were not conducted right after the wash fastness tests were finished. These findings further suggest that the actual penetration depth could be higher in all given cases, diminished by evaporative effects and exerting the biggest impact on the strand with the highest water exposure. Sodium dodecyl sulphate (SDS), a surfactant similar to SLES, is further known to promote the dissolution of AgNPs and slow down the reaction by complex formation with silver ions.[55] Furthermore, SDS-capped AgNPs were shown to cut the release of silver ions from the surface, thus prohibiting the formation of new AgNPs.[56,57] At this point, it remains unclear, to which extent SLES might have facilitated the distribution of AgNP precursors within the hair fibre in the first place and potentially caused a dissolution and subsequent relocation of the dye with ongoing washes, supported by the evaporation of water from the inside of the hair fibre.

The dissolution or movement of dye particles—either inwards or outwards—suggested that reversible interactions, covalent or non-covalent, formed between the hair fibre and the dye species, presumably resulting from charge interactions between functional groups of the keratin and silver ions released from the NPs' surface.[58,59] Introducing SLES to the system might have led to competing affinity with the hair fibre towards silver. The characteristic dye distribution pattern obtained could therefore be ascribed to different structures in the hair cortex, visualised by small, aggregated silver particles.[39]

Taking into account the critical molecular diameter for molecules to penetrate into the cuticula, the ability to move relatively freely inside the hair hinted to the existence of a species smaller than 6–8 Å (0.6–0.8 nm).[33] Thus, the formation of complexes between silver ions and polyphenols as source for the dye outcome could not be completely excluded at this point but seemed unlikely. Polyphenols especially interact with the hair cuticle, due to their size and functional groups. During complex formation the size of the resulting macromolecules increases and metal ions are immobilised.[22,23,60] Therefore, the movement of complexed ions into the cortex would be inhibited. A slight penetration of polyphenols into the cortex cannot be fully excluded for now, therefore, the determination of exact species inside the cortex is under current investigation.

3.5 | Assessment of hair damage caused by dyeing and subsequent washing

Healthy hair is desired by costumers but dyeing hair as well as combing and overall friction during washing can cause hair damage. Tensile strength investigations were conducted to assess the impact of the dyeing procedure as well as the subsequent washing on the hair fibre. Each 10 fibres of undyed, dyed as well as dyed and washed strands were investigated regarding the most important parameters, such as break stress, hair strain and Young's modulus. Mean values and SD are annexed in Table S2. All recorded stress–strain curves are annexed in Figure S4. Break stress describes the number of external forces required to cancel out the fibre's internal forces until failure,[61] taking into account the diameter of the hair fibre. Thus, a decrease in break stress can be indicative of mechanical or chemical hair damage. Neither dyeing nor subsequent washing had a significant impact on the hair strength as defined by break stress compared to an untreated fibre. No statistically significant difference ($p > 0.05$) was found between the three samples (Figure S5A). A significant increase in hair strain is considered an indicator for the breakage of cross-linkages within the hair,[33] resulting from chemical hair treatments. Neither dyeing nor subsequent washing had an impact on the hair strain ($p > 0.05$) (Figure S5B).

Another important parameter is the Young's modulus, calculated from the slope of the steepest region of the stress–strain curve, defining the hair strength in the elastic region of the hair fibre. Again, a decrease is linked to fibre damage.[34] Dyeing the hair according to the two-step method did not weaken the hair, as no statistically significant difference was found comparing the samples (Figure S5C). A slight difference ($p = 0.047$) was found comparing the dyed with the dyed and washed sample, indicating minor impact on the hair strength ascribed to the repeated washing, combing and blow-drying procedure.

Considering the findings, slight mechanical damage of the fibres from repeated washing and combing could have contributed to the observed redistribution effect of dye after 24 washes. Potential micron size cracks formed in the cuticle that reached down to the cortex enhanced the porosity and could thus have promoted the redistribution. On the contrary, no channelling of the dye was observed, that could indicate substantial blemishes in the structure of the hair fibre where the dye leaches out more easily.[62] As described, the relocation was even, in the form of concentric rings, accompanied by a homogenous dye impression. More mechanical strength data is required to gain a deeper understanding.

Furthermore, the overall chemical composition of the hair surface and the content of oxidation products from cysteine or cystin were taken into account as a chemical parameter for hair breakage due to the dyeing and washing process.[63] The results from XPS revealed no increase in oxidation products on the hair surface after dyeing and even further after washing compared to an undyed strand (Table S3). Likewise, the chemical composition of the hair surface regarding the most important elements carbon, nitrogen, oxygen and sulphur before and after dyeing revealed no change related to hair damage (Table S4). An increased nitrogen content on the hair surface was found after washing, probably related to the conditioning shampoo ingredient Guar hydroxypropyltrimonium chloride, a quaternary ammonium compound that attached to the fibre. Accordingly, no change in functional groups and chemical bonds on the hair surface was depicted before and after dyeing. The decrease in aliphatic carbon is again related to the adsorption of ingredients from the washing procedure (Table S5). FTIR investigations substantiated the findings, revealing a cysteic acid content at a constant level of 3–4% for all samples. Thus, dye-related hair damage as defined by the chemical composition or by oxidative products could not be validated.

3.6 | Investigation of isolated NP

The synthesis of AgNP was further confirmed using spectrophotometric and TEM measurements. During the reaction between RE solution and $AgNO_3$ a colour shift from pale yellow to intense red occurred under UV-visible irradiation (Figure 7B). The colour shift indicated the formation of AgNPs.[64] To further assess the synthesis of AgNPs, spectrophotometric analysis was used (Figure 7A). RE solution (yellow line) showed two absorption maxima at 266 and 332 nm, characteristic for flavonoids, for example, luteolin and apigenin, present inside the plant.[65,66] Furthermore, no significant absorption at the given concentration was found for $AgNO_3$ solution (light blue line).[67] The red solution of RE combined with $AgNO_3$ against UPW as baseline showed a peak at 450 nm in the spectrum (dark blue line). The peak became even more apparent using RE solution as baseline (violet line). The absorption could be attributed to the surface plasmon resonance (SPR) of AgNPs,[25,64,68–70] a phenomenon caused by the interaction of electromagnetic radiation with the surface conduction electrons of silver atoms. Due to that collective oscillation of electrons (surface plasmons) is induced, resulting in intense and brilliant colours.[68] Further evidence of the existence of AgNPs provided transmission electronic images from isolated NPs (Figure 7C). Biosynthesis led to the formation of spherical particles with a size distribution between 1 and 38 nm. Size and morphology were comparable to AgNPs of similar absorption maxima and colours as reported in the literature.[71]

Concluding from the overall observations, the following aspects need consideration for a proposal of dye mechanisms. The application of RE results in the deposition of polyphenols mainly on the hair cuticle due to their size. The reaction only takes place with either chloride or CA applied together with RE. After addition of $AgNO_3$ to the system and upon irradiation, the formation of NPs initiates. The formation of Ag-citrate complexes[72] as well as AgCl as intermediates seem probable as well, initiating the reaction in deeper layers of the fibre. The resulting NPs are presumed to subsequently diffuse (further) into the hair due to a suction effect resulting from charge interactions with hair's sulphur-moieties. At this point of research, the information regarding the role of the hair matrix in the formation of AgNPs are limited to the high affinity of silver towards sulphur-moieties inside the hair described in the literature and need further investigation.

In the absence of RE, using solely chloride, silver ions are assumed to precipitate as AgCl on the hair's surface as well as in the hair cortex, as described by Gummer,[39] followed by the reduction to AgNPs upon irradiation and the oxidation of chloride. It is conceivable that this reaction also occurs in the presence of RE. Despite its ability to penetrate the hair fibre,[73] the presumably insufficient reductive properties of citrate inhibit a respective reaction and the strands remain colourless when citrate is used exclusively.

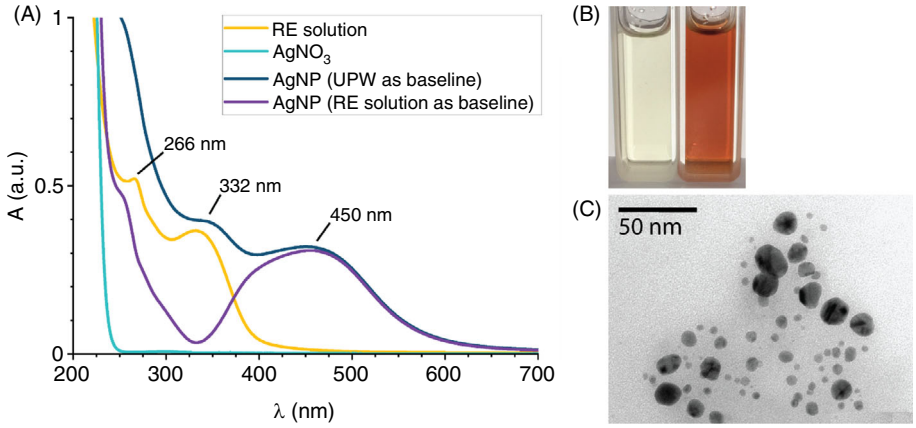


FIGURE 7 (A) UV-visible absorption spectra of RE solution (yellow) with absorption maxima at 266 and 332 nm, $AgNO_3$ solution (light blue) with both UPW as baseline. AgNP suspension using UPW (dark blue) as baseline reveals an additional absorption maximum at 450 nm originating from SPR of AgNPs. RE solution (violet) as baseline outlines the maximum due to removal of polyphenolic spectra. (B) Visual appearance of initial RE and $AgNO_3$ solution mixture (left) and after AgNP formation using UV-visible irradiation (right). (C) TEM micrograph of AgNP suspension revealing small spherical shaped AgNPs of different sizes ranging from 1 to 38 nm (black spots) surrounded by organic matter (dark grey spots).

Despite beneficial properties of AgNPs on dyeing intensity and wash fastness, the applicability of the proposed two-step hair dye method has to be evaluated regarding a potential impact on the human body as well as compliance with the Cosmetics Regulation. Compared to conventional routes to synthesise AgNPs, involving a plant extract supersedes a lot of harsh chemicals, such as sodium borohydride ($NaBH_4$). The demonstrated use case of in situ generated AgNPs is not tackled by the Cosmetics Regulation of the European Union (EU) No. 1223/2009, but the application of $AgNO_3$ is currently limited to eyebrows and eyelashes. Thus, more toxicological data as well as long-term studies are required to expand the field of application of $AgNO_3$ to the scalp.

Research results on toxicity of NPs and their ability to penetrate the skin reveal a size and shape dependency. Capped spherical AgNPs of 25 nm diameter were shown to enter several layers of the epidermis in humans,[74] and potentially the junctional parts to the dermis but without systemic absorption[75] when applied directly to the skin and incubated. A different study detected low levels of AgNPs in the dermis as well.[76] Hair shafts were found to play a special role as they constitute a hole in the skin where NPs can accumulate and penetrate into the skin more easily.[77] In animal tests, subsequent sensitisation or inflammation of the skin areal is reported,[78,79] presumably due to a release of ions from the NP's surface.[59] Yet, the dermal exposition is overall considered a low hazard.[80] The toxicity of AgNPs for aquatic ecosystems and fish, respectively, lies in the release of silver ions as well but is overall considered low as most studies depict the direct exposure of high concentrations towards fish, resulting in subsequent intoxications.[81]

The proposed two-step hair dye method is new and unique, based on the in situ generation of AgNPs inside keratinous fibres resulting in a high wash fastness. No significant dye-related hair damage was observed. The scarce research available describes the synthesis of NPs prior to the application to the hair fibre for dyeing purposes.[31] However, up to now, the method only allows the creation of one red shade, regardless of the different additives. It is known, that NPs exhibit different colours relative to their size and synthesis solvent,[82–84] therefore, a continuation of the method would potentially alter the colour impression on the hair as well. Since the penetration and hence systemic exposure of particles is size and shape dependent, a continuation could tackle both, new colours and consumer safety. Yet, it is debatable, if the surrounding hair matrix allows significantly bigger particles of different shapes, thus they could decrease the wash fastness. Silver-content of washed strands reveal that a high amount of silver persists on the hair. Reactions towards other trace-metal sensitive hair dyes are to be investigated in order to avoid exotherm reaction related injuries when re-dyeing the hair. Since $AgNO_3$ is a chemical sensitive to oxygen, the formulation of a stable cosmetic product might be challenging.

4 | CONCLUSION

We demonstrated a two-step method with subsequent UV-visible irradiation to achieve a red dye result on yak

hair fibres and underlined the importance of the pH adjustment using HCl or CA or the addition of NaCl during the first step. The best dye result was achieved with 1% aqueous RE suspension adjusted to pH 3 using HCl and subsequent treatment with 1% $AgNO_3$. Chloride-containing additives chosen for this work provoked the red dye formation in combination with $AgNO_3$ even without further addition of RE. Thus, the dye outcome was either achieved with chloride, regardless of the presence of RE or in an acidic milieu when RE was present. The evaluation of the method showed that the exposure time of the strand towards $AgNO_3$ could be reduced by almost 67% without a loss in dye intensity. A high wash fastness after 24 washes was demonstrated and further investigated via microscopic images of microtome cuts. An increasing penetration depth of the dye of up to 10% with ongoing wash cycles was observed. The red dye result could presumably be ascribed to in situ generation of AgNP in a redox-reaction of silver(I)-ions and polyphenols from RE, supported by UV-visible spectra of the recreated synthesis of AgNP in solution. The characteristic SPR-peak at 450 nm was observed.

ACKNOWLEDGEMENTS

Couleurs de Plantes (Rochefort, France) is kindly acknowledged for providing the *Reseda luteola* L. extract. The authors thank the electron microscopy unit of the University of Hamburg for TEM measurements. The authors would like to thank the service unit of Zentrale Element-Analytik of the University of Hamburg for the determination of the silver content in the samples. Swenja Kalischke (Henkel AG & Co. KGaA, Düsseldorf, Germany) is kindly acknowledged for her help and the preparation of microtome cuts. Yvonne Fellmer (Henkel AG & Co. KGaA, Düsseldorf, Germany) is kindly acknowledged for conducting the XPS and FTIR measurements. The authors wish to thank the Hamburgische Investitions-und Förderbank (IFB) for funding the project. Open Access funding enabled and organized by Projekt DEAL.

FUNDING INFORMATION

Investitions-und Förderbank Hamburg.

CONFLICT OF INTEREST STATEMENT

The authors declare no conflicts of interest.

DATA AVAILABILITY STATEMENT

The data that support the findings of this study are available from the corresponding author upon reasonable request.

ORCID

Julia K. Hachmann https://orcid.org/0009-0008-0872-5766
Jule M. Sauler https://orcid.org/0009-0000-1847-2629
Charlotte Ruhmlieb https://orcid.org/0000-0002-1685-9827
Volkmar Vill https://orcid.org/0000-0001-6527-9426
Fabian Straske https://orcid.org/0000-0003-4673-9647

REFERENCES

1. Dweck AC. Natural ingredients for colouring and styling. *Int J Cosmet Sci*. 2002;24:287-302.
2. Cui H, Cai R, Hua Z, Tang Y. Plant colorants for natural hair coloration: dyeing optimization and photostability assessment. *Sustain Chem Pharm*. 2023;36:2352-5541. doi:10.1016/j.scp.2023.101285
3. Ali S, Maqbool M, Hussain MT. Efficacy of some plants extracts for natural dyeing of human hair. *J Nat Fibers*. 2022;19(7):2581-2595. doi:10.1080/15440478.2020.1821280
4. Biertümpfel A, Wurl G. Dye plants in Europe. In: Bechtold T, Mussak R, eds. *Handbook of Natural Colorants*. Wiley; 2009:39-52.
5. Chong HP, Koh RY, Ng KY, Ng CH. Para-phenylenediamine containing hair dye: an overview of mutagenicity, carcinogenicity and toxicity. *J Environ Anal Toxicol*. 2016;6(5):1-6. doi:10.4172/2161-0525.1000403
6. Tkaczyk A, Mitrowska K, Posyniak A. Synthetic organic dyes as contaminants of the aquatic environment and their implications for ecosystems: a review. *Sci Total Environ*. 2020;717:1-19. doi:10.1016/j.scitotenv.2020.137222
7. Cui H, Xie W, Hua Z, et al. Recent advancements in natural plant colorants used for hair dye applications: a review. *Molecules*. 2022;27(22):8062. doi:10.3390/molecules27228062
8. Rust RC, Schlatter H. Hair Dyes. In: Draelos ZD, ed. *Cosmetic Dermatology: Products and Procedures*. 2nd ed. Wiley; 2016:239-250. doi:10.1002/9781118655566.CH28
9. Rose PM, Cantrill V, Benohoud M, Tidder A, Rayner CM, Blackburn RS. Application of anthocyanins from blackcurrant (Ribes nigrum L.) fruit waste as renewable hair dyes. *J Agric Food Chem*. 2018;66(26):6790-6798. doi:10.1021/acs.jafc.8b01044
10. Boga C, Delpivo C, Ballarin B, et al. Investigation on the dyeing power of some organic natural compounds for a green approach to hair dyeing. *Dyes Pigm*. 2013;97:9-18. doi:10.1016/j.dyepig.2012.11.020
11. Willemen H, van den Meijdenberg GJP, van Beek TA, Derksen GCH. Comparison of madder (Rubia tinctorum L.) and weld (Reseda luteola L.) total extracts and their individual dye compounds with regard to their dyeing behaviour, colour, and stability towards light. *Color Technol*. 2019;135(1):40-47. doi:10.1111/cote.12384
12. Ferreira ESB, Hulme AN, Mcnab H, Quye A. The natural constituents of historical textile dyes. *Chem Soc Rev*. 2004;33(6):329-336. doi:10.1039/b305697j
13. Melo MJ. History of natural dyes in the ancient Mediterranean world. In: Bechthold T, Mussak R, eds. *Handbook of Natural Colorants*. Wiley; 2009:3-20.
14. Vankar PS, Shukla D. Spectrum of colors from reseda luteola and other natural yellow dyes. *J Text Eng Fashion Technol*. 2018;4(2):106-119. doi:10.15406/jteft.2018.04.00127
15. Moiteiro C, Gaspar H, Rodrigues AI, Lopes JF, Carnide V. HPLC quantification of dye flavonoids in Reseda luteola L. from Portugal. *J Sep Sci*. 2008;31(21):3683-3687. doi:10.1002/jssc.200800383

16. Marques R, Sousa MM, Oliveira MC, Melo MJ. Characterization of weld (Reseda luteola L.) and spurge flax (Daphne gnidium L.) by high-performance liquid chromatography-diode array detection-mass spectrometry in Arraiolos historical textiles. *J Chromatogr A*. 2009;1216(9):1395-1402. doi:10.1016/j.chroma.2008.12.083
17. Safapour S, Mazhar M, Abedinpour S. Color shade extension of Reseda luteola L. natural colorant on wool textiles via binary combination of metal salts: colorimetric and fastness studies. *Fibers Polym*. 2023;24(9):3221-3233. doi:10.1007/s12221-023-00296-4
18. Jafari R, Gharanjig K, Hosseinnezhad M. Substitution of metal ion mordant with biomordants: effect on color and fastness of reseda dyed on wool yarns. *J Text I*. 2023;114(11):1623-1633. doi:10.1080/00405000.2022.2145427
19. Mesrar FE, Tachallait H, Bougrin K, Benhida R. Ultrasound-assisted extraction of vegetable dyes and mordants from wool dyed with Curcuma longa and Reseda luteola. *Ind Crops Prod*. 2024;208:1-12. doi:10.1016/j.indcrop.2023.117807
20. Barani H, Nasiri Boroumand M, Rafiei S. Application of silver nanoparticles as an antibacterial mordant in wool natural dyeing: synthesis, antibacterial activity, and color characteristics. *Fibers Polym*. 2017;18(4):658-665. doi:10.1007/s12221-017-6473-8
21. Geng H, Zhuang L, Li M, et al. Interfacial assembly of metal-phenolic networks for hair dyeing. *ACS Appl Mater Interfaces*. 2020;12(26):29826-29834. doi:10.1021/ACSAMI.0C06928
22. Jia D, Shen Y, Zhang X, Wang Y, Su R, Qi W. Colorful pigments based on multicomponent metal-phenol network nanoparticles for hair dyeing. *ChemistrySelect*. 2022;7(48):1-7. doi:10.1002/SLCT.202203886
23. Sargsyan L, Hippe T, Manneck H, Vill V. Tannin-mordant coloration with matcha (Camelia sinensis) and iron(II)-lactate on human hair tresses. *Molecules*. 2021;26(4):1-12. doi:10.3390/molecules26040829
24. Boroumand MN, Montazer M, Dutschk V. Biosynthesis of silver nanoparticles using Reseda Luteola L and their antimicrobial activity. *Ind Textila*. 2013;64(3):123-128.
25. Singh J, Dhaliwal AS. Novel green synthesis and characterization of the antioxidant activity of silver nanoparticles prepared from Nepeta leucophylla root extract. *Anal Lett*. 2018;52(2):213-230. doi:10.1080/00032719.2018.1454936
26. Pradeep M, Kruszka D, Kachlicki P, Mondal D, Franklin G. Uncovering the phytochemical basis and the mechanism of plant extract-mediated eco-friendly synthesis of silver nanoparticles using ultra-performance liquid chromatography coupled with a photodiode Array and high-resolution mass spectrometry. *ACS Sustain Chem Eng*. 2022;10(1):562-571. doi:10.1021/acssuschemeng.1c06960
27. Aboutorabi SN, Nasiriboroumand M, Mohammadi P, Sheibani H, Barani H. Preparation of antibacterial cotton wound dressing by green synthesis silver nanoparticles using mullein leaves extract. *J Renew Mater*. 2019;7(8):787-794. doi:10.32604/jrm.2019.06438
28. Im DS, Hong BM, Kim MH, Park WH. Formation of human hair-Ag nanoparticle composites via thermal and photo-reduction: a comparison study. *Colloids Surf A Physicochem Eng Asp*. 2020;600:1-7. doi:10.1016/j.colsurfa.2020.124995
29. Deng D, Gopiraman M, Kim SH, Chung IM, Kim IS. Human hair: a suitable platform for catalytic nanoparticles. *ACS Sustain Chem Eng*. 2016;4(10):5409-5414. doi:10.1021/ACSSUSCHEMENG.6B01689
30. Haveli SD, Walter P, Patriarche G, et al. Hair fiber as a nanoreactor in controlled synthesis of fluorescent gold nanoparticles. *Nano Lett*. 2012;12:6212-6217. doi:10.1021/nl303107w
31. Tang Y, Zhang Z, Yang S, Smith GJ, Liu L. Diatomite encapsulated AgNPs as novel hair dye cosmetics: preparation, performance, and toxicity. *Colloids Surf B Biointerfaces*. 2021;200:1-10. doi:10.1016/j.colsurfb.2021.111599
32. Brainard DH. The science of color. In: Shevell SK, ed. *Color Appearance and Color Difference Specification*. 1st ed. Elsevier Science; 2003:191-216 Accessed May 14, 2024. http://munsell.com/
33. Robbins CR. *Chemical and Physical Behavior of Human Hair*. 5th ed. Springer; 2012. doi:10.1007/978-3-642-25611-0
34. Cameron GJ, Wess TJ, Bonser RHC. Young's modulus varies with differential orientation of keratin in feathers. *J Struct Biol*. 2003;143(2):118-123. doi:10.1016/S1047-8477(03)00142-4
35. King ME, Kent IA, Personick ML. Halide-assisted metal ion reduction: emergent effects of dilute chloride, bromide, and iodide in nanoparticle synthesis. *Nanoscale*. 2019;11:15612-15621. doi:10.1039/c9nr04647j
36. Singh A, Hou WC, Lin TF, Zepp RG. Roles of silver−chloride complexations in sunlight-driven formation of silver nanoparticles. *Environ Sci Technol*. 2019;53:11162-11169. doi:10.1021/acs.est.9b02115
37. Yin Y, Xu W, Tan Z, et al. Photo-and thermo-chemical transformation of AgCl and Ag 2 S in environmental matrices and its implication. *Environ Pollut*. 2017;220:955-962. doi:10.1016/j.envpol.2016.10.081
38. Dong L, Liang D, Gong R. In situ photoactivated AgCl/Ag nanocomposites with enhanced visible light photocatalytic and antibacterial activity. *Eur J Inorg Chem*. 2012;2012(19):3200-3208. doi:10.1002/EJIC.201200172
39. Gummer CL. Elucidating penetration pathways into the hair fiber using novel microscopic techniques. *J Cosmet Sci*. 2001;52:265-280.
40. Restrepo CV, Villa CC. Synthesis of silver nanoparticles, influence of capping agents, and dependence on size and shape: a review. *Environ Nanotechnol Monit Manag*. 2021;15(100428):1-15. doi:10.1016/j.enmm.2021.100428
41. Singh A, Sharma B, Deswal R. Green silver nanoparticles from novel Brassicaceae cultivars with enhanced antimicrobial potential than earlier reported Brassicaceae members. *J Trace Elem Med Biol*. 2018;47:1-11. doi:10.1016/j.jtemb.2018.01.001
42. Henglein A, Giersig M. Formation of colloidal silver nanoparticles: capping action of citrate. *J Phys Chem B*. 1999;103:9533-9539. doi:10.1021/jp9925334
43. Shi AM, Li D, Wang LJ, Adhikari B. The effect of NaCl on the rheological properties of suspension containing spray dried starch nanoparticles. *Carbohydr Polym*. 2012;90(4):1530-1537. doi:10.1016/j.carbpol.2012.07.025
44. Martin JJ, Cardamone JM, Irwin PL, Brown EM. Keratin capped silver nanoparticles - synthesis and characterization of a nanomaterial with desirable handling properties. *Colloids Surf B Biointerfaces*. 2011;88(1):354-361. doi:10.1016/j.colsurfb.2011.07.013
45. Lü X, Cui S. Wool keratin-stabilized silver nanoparticles. *Bioresour Technol*. 2010;101(12):4703-4707. doi:10.1016/j.biortech.2010.01.110

46. Bate LC. Adsorption and elution of trace elements on human hair*. *Int J Appl Radiat Isot*. 1966;17:417-423. doi:10.1016/0020-708X(66)90068-8
47. Simpson WS, Mason PCR. Absorption of silver ions by wool. *Text Res J*. 1969;39:434-441.
48. Popescu C, Höcker H. Hair-the most sophisticated biological composite material. *Chem Soc Rev*. 2007;36:1282-1291. doi:10.1039/b604537p
49. Müllner ARM, Pahl R, Brandhuber D, Peterlik H, Lichtenegger H, Rennhofer H. Porosity at different structural levels in human and yak belly hair and its effect on hair dyeing. *Molecules*. 2020;25(2143):2143. doi:10.3390/molecules25092143
50. Bontozoglou C, Zhang X, Patel A, Lane ME, Xiao P. In vivo human hair hydration measurements by using Opto-thermal radiometry. *Int J Thermophys*. 2019;40(22):1-11. doi:10.1007/s10765-018-2477-x
51. Wortmann FJ, Gotschey M, Schmidt-Lewerkühne H. Diffusion and distribution of element-labelled surfactants in human hair. *Int J Cosmet Sci*. 2004;26:61-69. doi:10.1111/j.0412-5463.2004.00204.x
52. Molleman B, Hiemstra T. Surface structure of silver nanoparticles as a model for understanding the oxidative dissolution of silver ions. *Langmuir*. 2015;31:13361-13372. doi:10.1021/acs.langmuir.5b03686
53. Fuse N, Matsui M, Matsue Y. Temporal and spatial visualization of water uptake into human hair studied by infrared microscopy. *Anal Sci*. 2022;38:601-605. doi:10.1007/s44211-022-00074-x
54. Lee Y, Kim YD, Hyun HJ, Pi LQ, Jin X, Lee WS. Hair shaft damage from heat and drying time of hair dryer. *Ann Dermatol*. 2011;23(4):455-462. doi:10.5021/ad.2011.23.4.455
55. Pal T, Sau TK, Jana NR. Reversible formation and dissolution of silver nanoparticles in aqueous surfactant media. *Langmuir*. 1997;13(6):1481-1485. doi:10.1021/LA960834O
56. Shah V, Bharatiya B, Mishra MK, Ray D. Molecular insights into sodium dodecyl sulphate mediated control of size for silver nanoparticles. *J Mol Liq*. 2019;273:222-230. doi:10.1016/j.molliq.2018.10.042
57. AL-Thabaiti SA, Al-Nowaiser FM, Obaid AY, Al-Youbi AO, Khan Z. Formation and characterization of surfactant stabilized silver nanoparticles: a kinetic study. *Colloids Surf B Biointerfaces*. 2008;67(2):230-237. doi:10.1016/j.colsurfb.2008.08.022
58. Nikiforova T, Kozlov V, Islyaikin M. Sorption of d-metal cations by keratin from aqueous solutions. *J Environ Chem Eng*. 2019;7(5):103417. doi:10.1016/j.jece.2019.103417
59. Danscher G, Locht LJ. In vivo liberation of silver ions from metallic silver surfaces. *Histochem Cell Biol*. 2010;133:359-366. doi:10.1007/s00418-009-0670-5
60. Jin L, Yun D, Zhang W, et al. Polyphenols coordinated with Cu (II) in an aqueous system build Ion-Channel coatings on hair surfaces. *Materials*. 2023;16(4):1333. doi:10.3390/ma16041333
61. Davis MG, Thomas JH, Van De Velde S, et al. A novel cosmetic approach to treat thinning hair funding sources. *Br J Dermatol*. 2011;165:24-30. doi:10.1111/j.1365-2133.2011.10633.x
62. Zhang G, McMullen RL, Kulcsar L. Investigation of hair dye deposition, hair color loss, and hair damage during multiple oxidative dyeing and shampooing cycles. *J Cosmet Sci*. 2016;67:1-11.
63. Inoue T, Takehara K, Shimizu N, Kitajima Y, Shinohara K, Ito A. Application of XANES profiles to X-ray spectromicroscopy for biomedical specimens: part II. Mapping oxidation state of cysteine in human hair. *J Xray Sci Technol*. 2011;19:313-320. doi:10.3233/XST-2011-0295
64. Mittal AK, Bhaumik J, Kumar S, Banerjee UC. Biosynthesis of silver nanoparticles: elucidation of prospective mechanism and therapeutic potential. *J Colloid Interface Sci*. 2014;415:39-47. doi:10.1016/J.JCIS.2013.10.018
65. Raji Y, Nadi A, Chemchame Y, et al. Eco-friendly extraction of flavonoids dyes from Moroccan (Reseda luteola L.), wool dyeing, and antibacterial effectiveness. *Fibers Polym*. 2023;24(3):1051-1065. doi:10.1007/s12221-023-00019-9
66. Rice-Evans CA, Miller NJ, Paganga G. Structure-antioxidant activity relationships of flavonoids and phenolic acids. *Free Radic Biol Med*. 1996;20(7):933-956. doi:10.1016/0891-5849(95)02227-9
67. Kundu S, Wang K, Liang H. Size-controlled synthesis and self-assembly of silver nanoparticles within a minute using microwave irradiation. *J Phys Chem C*. 2009;113(1):134-141. doi:10.1021/JP808292S
68. Krajczewski J, Koła K, Kudelski A. Plasmonic nanoparticles in chemical analysis. *RSC Adv*. 2017;7(28):17559-17576. doi:10.1039/c7ra01034f
69. Martínez-Castañón GA, Niño-Martínez N, Martínez-Gutierrez F, Martínez-Mendoza JR, Ruiz F. Synthesis and antibacterial activity of silver nanoparticles with different sizes. *J Nanopart Res*. 2008;10(8):1343-1348. doi:10.1007/s11051-008-9428-6
70. Kasthuri J, Kathiravan AK, Rajendiran AN. Phyllanthin-assisted biosynthesis of silver and gold nanoparticles: a novel biological approach. *J Nanopart Res*. 2009;11:1075-1085. doi:10.1007/s11051-008-9494-9
71. Rivero PJ, Goicoechea J, Urrutia A, Arregui FJ. Effect of both protective and reducing agents in the synthesis of multicolor silver nanoparticles. *Nanoscale Res Lett*. 2013;8:101. doi:10.1186/1556-276X-8-101
72. Patra S, Pandey AK, Sen D, et al. Redox decomposition of silver citrate complex in nanoscale confinement: an unusual mechanism of formation and growth of silver nanoparticles. *Langmuir*. 2014;30(9):2460-2469. doi:10.1021/LA4048787
73. Zhang D, Baghdadli N, Greaves AJ. Reinforcing chemically treated human hair with citric acid. *Int J Cosmet Sci*. 2025;47(3):1. doi:10.1111/ICS.13039
74. Larese FF, D'agostin F, Crosera M, et al. Human skin penetration of silver nanoparticles through intact and damaged skin. *Toxicology*. 2009;255:33-37. doi:10.1016/j.tox.2008.09.025
75. George R, Merten S, Wang TT, Kennedy P, Maitz P. In vivo analysis of dermal and systemic absorption of silver nanoparticles through healthy human skin. *Australas J Dermatol*. 2014;55(3):185-190. doi:10.1111/AJD.12101
76. Bianco C, Adami G, Crosera M, et al. Silver percutaneous absorption after exposure to silver nanoparticles: a comparison study of three human skin graft samples used for clinical applications. *Burns*. 2014;40(7):1390-1396. doi:10.1016/j.burns.2014.02.003
77. Lademann J, Richter H, Teichmann A, et al. Nanoparticles - an efficient carrier for drug delivery into the hair follicles. *Eur J Pharm Biopharm*. 2007;66(2):159-164. doi:10.1016/j.ejpb.2006.10.019
78. Samberg ME, Oldenburg SJ, Monteiro-Riviere NA. Evaluation of silver nanoparticle toxicity in skin in vivo and keratinocytes

in vitro. *Environ Health Perspect*. 2010;118(3):407-413. doi:10.1289/ehp.0901398
79. Kazem Koohi M, Hejazy M, Asadi F, Asadian P. Assessment of dermal exposure and histopathologic changes of different sized nano-silver in healthy adult rabbits. *J Phys: Conf Ser*. 2011;304:12028. doi:10.1088/1742-6596/304/1/012028
80. Hadrup N, Sharma AK, Loeschner K. Toxicity of silver ions, metallic silver, and silver nanoparticle materials after in vivo dermal and mucosal surface exposure: a review. *Regul Toxicol Pharmacol*. 2018;98:257-267. doi:10.1016/j.yrtph.2018.08.007
81. Callaghan NI, MacCormack TJ. Ecophysiological perspectives on engineered nanomaterial toxicity in fish and crustaceans. *Comp Biochem Physiol C Toxicol Pharmacol*. 2017;193:30-41. doi:10.1016/j.cbpc.2016.12.007
82. Zielinska A, Skwarek E, Zaleska A, Gazda M, Hupka J. Preparation of silver nanoparticles with controlled particle size. *Procedia Chem*. 2009;1:1560-1566. doi:10.1016/j.proche.2009.11.004
83. Tang B, Li J, Hou X, Afrin T, Sun L, Wang X. Colorful and antibacterial silk fiber from anisotropic silver nanoparticles. *Ind Eng Chem Res*. 2013;52(12):4556-4563. doi:10.1021/IE3033872
84. Wu M, Ma B, Pan T, Chen S, Sun J. Silver-nanoparticle-colored cotton fabrics with tunable colors and durable antibacterial and self-healing superhydrophobic properties. *Adv Funct Mater*. 2016;26(4):569-576. doi:10.1002/ADFM.201504197

SUPPORTING INFORMATION

Additional supporting information can be found online in the Supporting Information section at the end of this article.

How to cite this article: Hachmann JK, Sauler JM, Ruhmlieb C, Vill V, Straske F. Red era: Dyeing yak hair fibres red with in situ generated silver nanoparticles using silver nitrate and a flavonoid-containing plant extract. *Coloration Technology*. 2026;142(3):439-455. doi:10.1111/cote.70007